2013

Spectral Modulation through Controlling Anions in Nanocaged Phosphors

Hongyu Bian
Northeast Normal University

Yuxue Liu
Northeast Normal University

Duanting Yan
Northeast Normal University

Hancheng Zhu
Northeast Normal University

Chunguang Liu
Northeast Normal University

See next page for additional authors

Journal of Materials Chemistry C

RSC Publishing

PAPER

View Article Online
View Journal | View Issue

Cite this: J. Mater. Chem. C, 2013, 1, 7896

Spectral modulation through controlling anions in nanocaged phosphors

Hongyu Bian,[a] Yuxue Liu,*[a] Duanting Yan,[a] Hancheng Zhu,[a] Chunguang Liu,[a] Changshan Xu,[a] Yichun Liu,[a] Hong Zhang*[b] and Xiaojun Wang*[c]

Received 25th July 2013
Accepted 2nd October 2013

DOI: 10.1039/c3tc31446d

www.rsc.org/MaterialsC

A new approach has been proposed and validated to modulate the emission spectra of europium-doped $12CaO \cdot 7Al_2O_3$ phosphors by tuning the nonradiative and radiative transition rates, realized by controlling the sort and amount of the encaged anions. A single wavelength at 255 nm can excite simultaneously Eu^{2+} and Eu^{3+} centres to yield blue and red emissions, respectively. The amount of the anions in the nanocages, like OH^- and H^-, can be controlled by heat treatment processes. The existence of encaged OH^- accelerates the nonradiative process of the emission centres, while the presence of encaged H^- induces a higher symmetry that decreases the radiative transition rate, confirmed by the analysis of decay processes. It is demonstrated that the emission colour is tuned finely from red to blue with the CIE chromaticity coordinates from (0.630, 0.352) to (0.216, 0.086) when the annealing time increases. This strategy can be readily extended to similar systems with other rare earth active centres.

1. Introduction

Recently, light-emitting diodes (LEDs) are of interest in terms of energy efficiency and practical advantages compared to conventional bulbs and phosphorescent tubes.[1–5] A new strategy, involving a mixed valence europium activated phosphor under a single wavelength excitation, has been proposed to overcome many drawbacks of conventional means of white light generation for LEDs, such as low device efficiency and colour rendering index.[6,7] Because Eu^{2+} and Eu^{3+} emit in different spectral regions, modulation of the luminescence of a mixed valence europium phosphor has been realized mainly through varying the concentration ratio of Eu^{3+} to Eu^{2+}. For instance, Li is introduced into $Eu_{0.33}Zr_2(PO_4)_3$ system to enhance the reduction of Eu^{3+} based on the charge compensation.[8–11] In another case, replacing Al^{3+}–F^- by the appropriate dopant Si^{4+}–O^{2-} in $Ca_{12}Al_{14}O_{32}F_2$ is adopted to enable Eu^{3+} to be converted to Eu^{2+} due to enlarging the activator site.[12] The emission spectrum also relies on the relevant nonradiative and radiative transition rates. Considering the fact that there is no report for Eu doped phosphors on this aspect, the ability of tuning the local environments of Eu^{3+} and Eu^{2+} to modulate the rates and therefore the luminescence of a mixed valence europium phosphor offers a new approach to adjusting the colour of phosphors.

$12CaO \cdot 7Al_2O_3$ (C12A7) is a unique material that possesses a nanocaged structure, as shown in Fig. 1. The unit cell consists of 12 cages forming the positively charged framework and two free O^{2-} occupying randomly 2 of the 12 cages to maintain the charge neutrality.[13] The free O^{2-} ions can be replaced by other

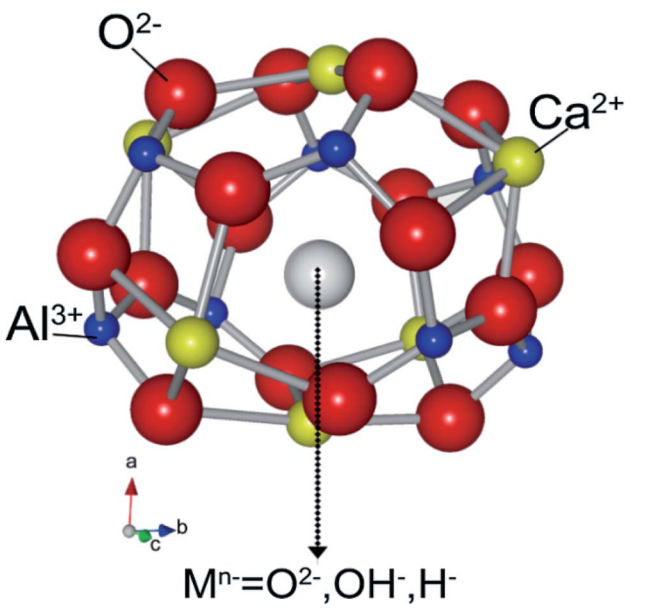

Fig. 1 The nanocage structure of C12A7.

[a]Centre for Advanced Optoelectronic Functional Materials Research & Key Laboratory for UV Light-Emitting Materials and Technology of the Ministry of Education, Northeast Normal University, 5268 Renmin Street, Changchun 130024, China. E-mail: yxliu@nenu.edu.cn; Fax: +86-0431-85099851; Tel: +86-0431-85099851

[b]Van't Hoff Institute for Molecular Sciences, University of Amsterdam, P.O. Box 94157, 1090 GD Amsterdam, The Netherlands. E-mail: H.Zhang@uva.nl; Fax: +31-20-5255604; Tel: +31-20-5256976

[c]Department of Physics, Georgia Southern University, Statesboro, GA 30460-8031, USA. E-mail: xwang@georgiasouthern.edu; Fax: +1-912-478-0471; Tel: +1-912-478-5503

anions, like OH^- and H^-,[14] where OH^- could accelerate the nonradiative process of the emission centres around it because of its high frequency vibration. In the meantime, the radiative transition rate is closely related to the local symmetry of the emission centres. Deformation of the cages can be induced through the encaged anions in C12A7 and its degree may therefore be adjusted by the sort of anions. The larger the induced deformation is, the lower the symmetry created,[15] and thus the radiative transition rates are modified.

In this work, we have proposed an approach to modulate the luminescence of mixed valence europium doped C12A7 (C12A7:Eu) by tuning the nonradiative and radiative transition rates, realized by controlling the sort and amount of the encaged anions. The nonradiative transition rates of Eu^{3+} are modified by encaged OH^-, whereas the radiative transition rates of Eu^{2+} are tuned by encaged H^-. The CIE chromaticity coordinates are tuned from red region (0.630, 0.352) to blue region (0.216, 0.086). Superior to the other mixed valence europium phosphors, Eu^{3+} is easily converted to Eu^{2+} with the help of the nanocages and encaged O^{2-} ions in C12A7. On the other hand, the allowed charge transfer excitation of Eu^{3+} in this work is much more efficient than that of forbidden f → f transitions excitation.[6,7,16] The insight gained from this work may provide a new mechanism for designing LEDs and novel optical materials.

2. Experimental

A self-propagating combustion method was adopted to synthesize C12A7:x%Eu^{3+} (x = 0.1, 0.5 and 1.0) powders. $Ca(NO_3)_2 \cdot 4H_2O$ (99.99%), $Al(NO_3)_3 \cdot 9H_2O$ (99.99%), $Eu(NO_3)_3 \cdot 6H_2O$ (99.99%), urea, and β-alanine were used as starting materials and dissolved in deionized water according to the proposed metal mole ratio in C12A7:x%Eu^{3+} with Eu^{3+} ions substituting Ca^{2+} ions. Combustion of the metal nitrate, urea, and β-alanine solution was performed in a tub container in a preheated furnace. The precursor solution turned to a yellow-white gel as solvent was evaporated and then spontaneous ignition occurred, yielding pale-white ashes. The resultant ashes were then collected and calcined in air at 1000 °C for 6 h to remove any carbon residues remaining in the oxide powders. The resultant C12A7:0.5%Eu^{3+} powders were annealed in a 20% H_2/80% N_2 atmosphere at 1300 °C for 2, 4 and 9 h to modulate the luminescence *via* the variation of the content ratio of Eu^{3+}/Eu^{2+}, the radiative and nonradiative transitions rates. H^- and OH^- were introduced into the nanocages as described in the following reaction:

$$H_2(g) + O^{2-}(c) = H^-(c) + OH^-(c), \quad (1)$$

where (c) and (g) specify the species in the cage and the gas phase, respectively.[13] To study if the spectrum can be modulated, the samples were then annealed in air at 400 °C for 0.33 h.

The crystal structures of mixed valence europium doped C12A7 powders were examined by a Rigaku D/max-RA X-ray diffraction (XRD) spectrometer using Cu Kα radiation (line of 0.15418 nm). The microstructures of C12A7:Eu powders were investigated by means of a scanning electron microscope (SEM, FEI, Quanta FEG 250). The photoluminescence (PL) and photoluminescence excitation (PLE) spectra were recorded with a SHIMADZU RF-5301PC spectrofluorometer. The Fourier Transform IR (FTIR) transmittance spectra were taken with a Nicolet 6700 Fourier Transform Infrared Spectrometer. The powders are mixed with KBr at a weight ratio of 3 : 100 and then ground and pressed at a pressure of 20 MPa to obtain pellets. The absolute quantum yield was analyzed with a PL quantum-efficiency measurement system (C9920-02, Hamamatsu Photonics). Diffuse reflectance spectra were taken using a Lambda 900 UV/VIS/NIR spectrophotometer (Perkin Elmer, USA). The luminescence decays were taken with a 600 MHz LeCroy digital oscilloscope upon the excitation of different wavelengths from an optical parametric oscillator. All the above experiments were tested at room temperature.

3. Results and discussion

A single phase of C12A7 (JCPDS: 09-0413) with Eu^{3+} concentration lower than 0.5% is confirmed by the XRD patterns of C12A7:x%Eu^{3+} shown in Fig. 2. When the concentration is above 0.5% other phases emerge, C12A7:0.5%Eu^{3+} is therefore chosen for the following studies. Eu^{3+} ions substitute Ca^{2+} ions in C12A7 since the radius of Eu^{3+} ion, 0.95 Å, is comparable with that of Ca^{2+} (0.99 Å) but much larger than the Al^{3+} (0.39 Å).

The emission and excitation spectra of the as-prepared C12A7:0.5%Eu^{3+} are shown in Fig. 3a and b, respectively. The emission spectrum, under the excitation of 255 nm, exhibits two major peaks centred at 586 and 616 nm, resulting from the magnetic dipole transition $^5D_0 \rightarrow {}^7F_1$ and electronic dipole transition $^5D_0 \rightarrow {}^7F_2$ of Eu^{3+}, respectively.[17] In the excitation spectrum, a broad band in the 220–280 nm range and several

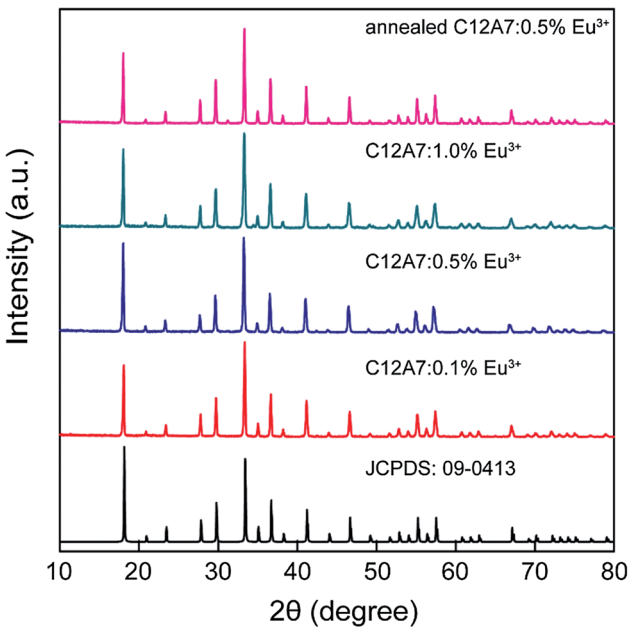

Fig. 2 XRD of C12A7:x%Eu^{3+} (x = 0.1, 0.5, 1.0) and C12A7:0.5%Eu^{3+} annealed in H_2/N_2 atmosphere.

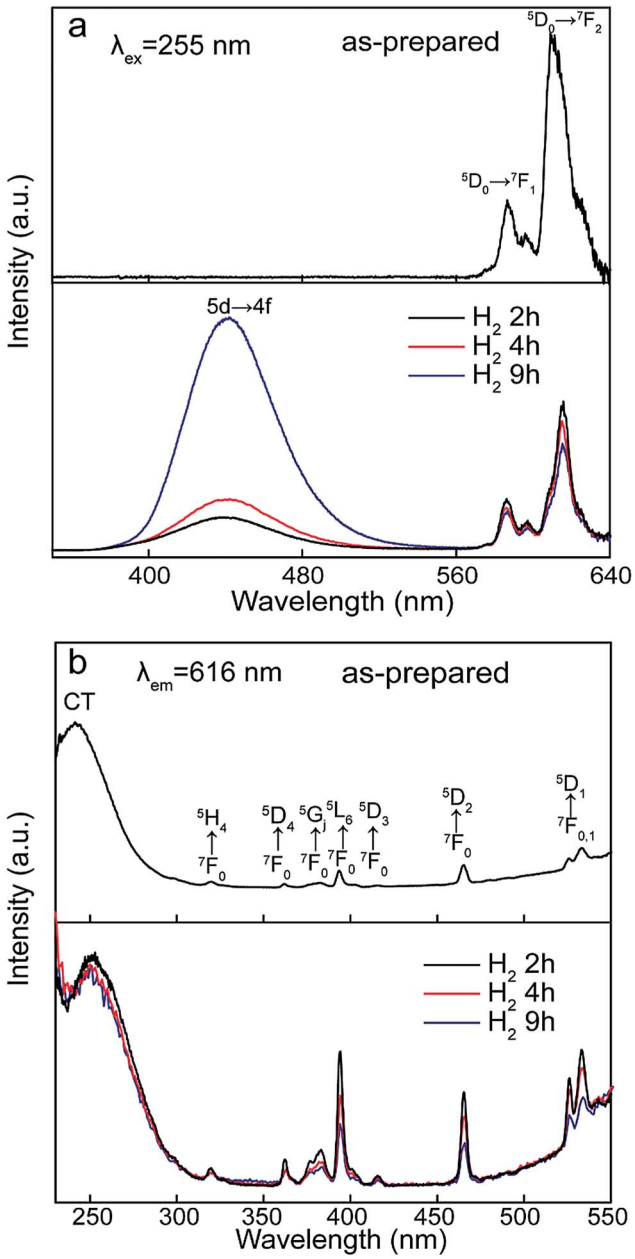

Fig. 3 (a) Emission (λ_{ex} = 255 nm) and (b) excitation (λ_{em} = 616 nm) spectra of the as-prepared and the annealed samples.

sharp peaks in the 310–480 nm range appear when 616 nm emission wavelength ($^5D_0 \rightarrow {}^7F_2$ transition of Eu^{3+}) is monitored. The broad band is assigned to the $O_{2p} \rightarrow Eu_{4f}$ charge transfer (CT) transition,[18] whereas the sharp peaks at 320, 362, 383, 394, 415, 465, 526 and 533 nm correspond to transitions from the $^7F_0$ or $^7F_1$ ground state to the $^5H_4$, $^5D_4$, ^5G_J, $^5L_6$, $^5D_3$, $^5D_2$ and $^5D_1$ states of Eu^{3+}, respectively.[16,19] The CT excitation band is found to be much stronger than the characteristic transitions of Eu^{3+}, verifying that it is a more efficient excitation channel to achieve the red emission.

To modulate the colour through controlling the anions in the nanocages, the as-prepared sample is annealed in a H_2/N_2 atmosphere. The annealed samples retain the C12A7 phase, confirmed by the XRD pattern shown in Fig. 2. Grain sizes of the as-prepared and the annealed samples are determined to be 300–500 nm and 1.5–2.5 μm, respectively, by the SEM images (Fig. 4a and b). The smaller grain size of the as-prepared sample is helpful for the H^- and OH^- substitution for the encaged O^{2-} because the reaction described by eqn (1) happens only on the surface of particles as reported by Hayashi *et al.*[20,21] and Ruszak *et al.*[22] Their works suggested that the hydrides and the protons as mono-atomic species can penetrate into the nanocages. In the meantime, the absorption spectra in the visible region are recorded, which demonstrate that the treatment to the samples barely changes their colour and no excessive reduction happens, even if the as-prepared sample is annealed in H_2 atmosphere for 9 h.

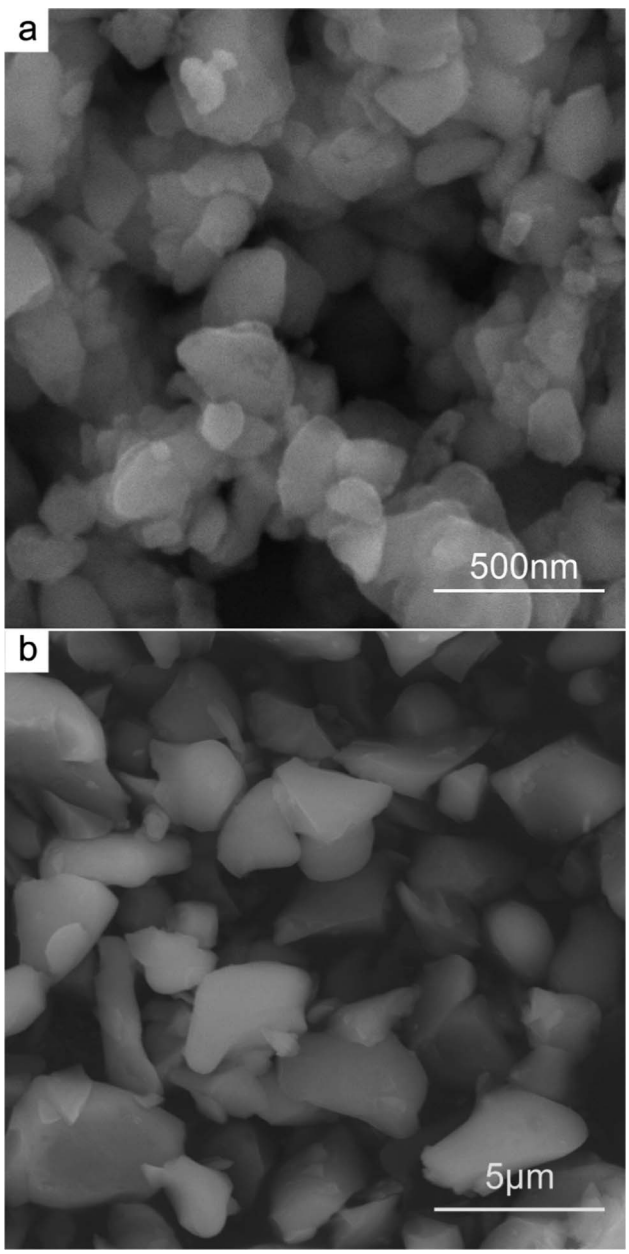

Fig. 4 SEM images of (a) the as-prepared sample and (b) C12A7:0.5%Eu^{3+} annealed in H_2/N_2 atmosphere.

Under the excitation of 255 nm, emissions of C12A7:Eu with different annealing times shown in Fig. 3a are found in the ranges of 400–500 nm (blue) and 570–630 nm (red), ascribed to Eu^{2+} and Eu^{3+}, respectively. Excitation responsible for the 616 nm emission of Eu^{3+} is observed in the regions of 220–280 (broad band) and 310–480 nm (sharp peaks) and there is no significant change to the excitation spectra after annealing, as shown in Fig. 3b. When the 438 nm emission of Eu^{2+} is monitored, however, two broad absorption bands are observed in the ranges of 240–280 and 280–400 nm, originating from the 4f–5d transitions of Eu^{2+} ions as shown in Fig. 5a. Based on the (distorted) octahedral symmetry of the doped Eu sites in C12A7, the former is assigned to $4f^7$ ($^8S_{7/2}$) → $4f^65d^1$ (e_g) and the latter to $4f^7$ ($^8S_{7/2}$) → $4f^65d^1$ (t_{2g}).[23–26] The allowed and efficient excitation for both Eu^{2+} (220–280 nm) and Eu^{3+} (240–280 nm) overlaps in the region of 240–280 nm, indicating that the two ions can be simultaneously excited with a single wavelength UV light to yield both blue and red emissions.

Fig. 3a depicts the annealing effect on the spectra, where the luminescence of Eu^{2+} is found to increase greatly, whereas that of Eu^{3+} decreases slightly, with the annealing time varying from 2 to 9 h. This observation can be related to the following factors during the annealing: (i) some Eu^{3+} ions are converted to Eu^{2+}, (ii) the amount of high frequency vibrational groups in the nanocages, like OH^-, increases and (iii) the amount of other ions in the nanocages, like H^-, also increases, as described by eqn (1). Factor (i) tunes the luminescence by increasing the ratio of Eu^{2+} to Eu^{3+} centres. Factor (ii) can accelerate the non-radiative process of the emission centres next to OH^- because of its high frequency vibration. Meanwhile, the higher symmetry is created by factor (iii) due to the reduced deformation of nanocages induced by more OH^- and H^-. The deformation can be measured by the Ca–Ca distance of the cage, d_{Ca-Ca}, which is close to 5.77 Å for the empty cages and decreases to 4.93 Å and 4.27 Å when the cages are occupied by monovalent (H^-, OH^-) and divalent anions (O^{2-}), respectively.[27,28] The larger d_{Ca-Ca} that is measured, the less the deformation induced, and thus the higher symmetry created. Especially, the integrated intensity ratio of the $^5D_0$–$^7F_2$ to $^5D_0$–$^7F_1$ emissions of Eu^{3+} becomes smaller as the symmetry of Eu sites in C12A7 becomes higher because of the hypersensitivity of the former.[17] Indeed, the ratio is found decreased from 4.0 for as-prepared sample to 2.7 for the H_2 annealed sample confirming the above theoretical predictions. In addition, when monitoring the 438 nm emission of Eu^{2+}, red- and blue-shifts of excitations at 255 and 326 nm, respectively, are observed after the annealing (Fig. 5a), and the red shift of the emission peak with the increasing H_2 annealing time can be seen under excitation of 255 nm (Fig. 5b). Usually, 5d orbital splitting depends on its local crystal field and it becomes narrower when the crystal field gets weaker. This is verified by our observation, suggesting that a weaker local crystal field is created due to less deformation.

In order to unravel the relation between the luminescence and encaged anions, we now study the dynamic processes in Eu^{3+} and Eu^{2+}. Fig. 6 shows the luminescence decays of the $^5D_0$ → $^7F_2$ transition of Eu^{3+} monitored at 616 nm and the fitting results are listed in Table 1. All the decays of Eu^{3+} can be sorted into two components, reflecting that Eu^{3+} ions have two different environments. One has O^{2-} in the vicinity, having a relatively long decay time, and the other has encaged OH^- around with a short decay time. After the annealing, more OH^- anions are generated following the reaction described by eqn (1) and diffused into the neighbours of the two sorts of Eu^{3+} emission centres. Thus, the lifetimes of the long and short components decrease from 1.20 and 0.37 ms to 0.87 and

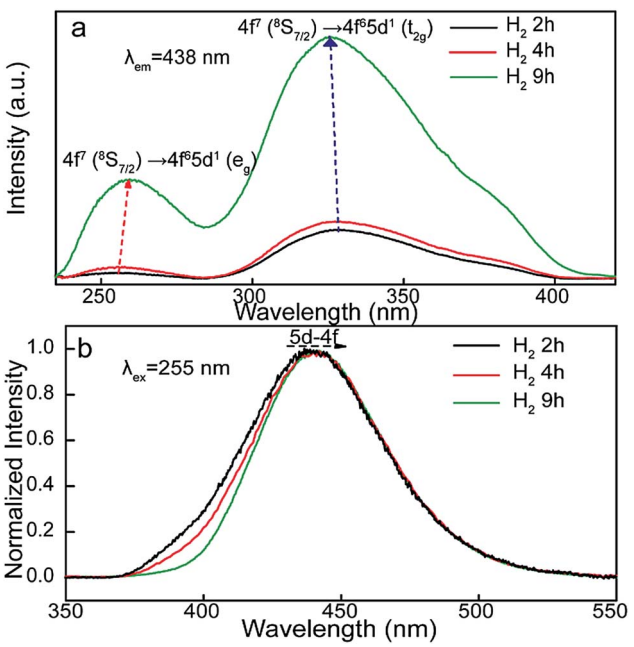

Fig. 5 (a) Excitation spectra (λ_{em} = 438 nm) and (b) normalized emission (λ_{ex} = 255 nm) spectra of C12A7:0.5%Eu^{3+} annealed in H_2/N_2 atmosphere for different times.

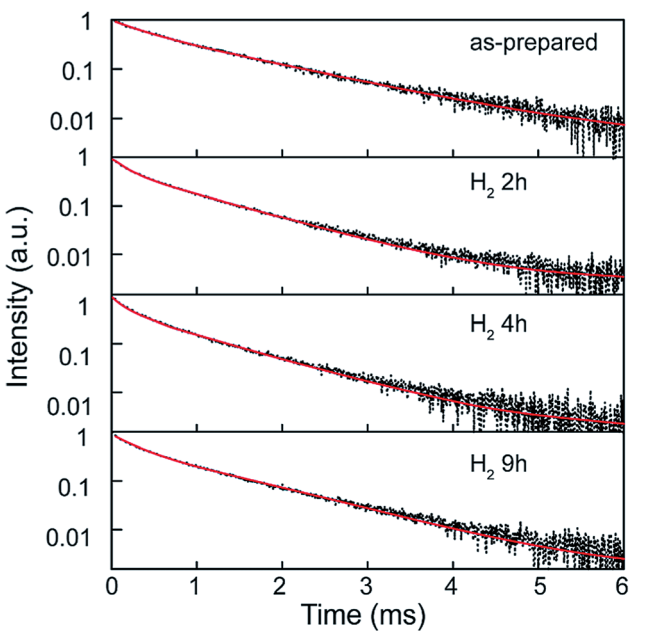

Fig. 6 Decay curves of Eu^{3+} monitored at 616 nm and excited at 255 nm. The red line represents the data best fit using a bi-exponential function.

Table 1 Bi-exponential fitting parameters of the emissions under 255 nm excitation and the quantum yields of C12A7:Eu under different conditions

Sample[a]	Heating (h) (H_2 or air)	Decay[b] (ms) (616 mm)	Decay[c] (μs) (438 nm)	Quantum yield[d]
a	As-prepared	$\tau_1 = 0.37$ (35.7%) $\tau_2 = 1.20$ (64.3%)	—	12.7%
b	2, H_2	$\tau_1 = 0.18$ (44.7%) $\tau_2 = 0.89$ (55.3%)	$\tau_1 = 0.84$ (54.9%) $\tau_2 = 5.45$ (45.1%)	12.8%
c	4, H_2	$\tau_1 = 0.18$ (47.3%) $\tau_2 = 0.87$ (52.7%)	$\tau_1 = 0.85$ (39.0%) $\tau_2 = 4.93$ (61.0%)	29.4%
d	9, H_2	$\tau_1 = 0.23$ (41.2%) $\tau_2 = 1.00$ (58.8%)	$\tau_1 = 1.14$ (20.0%) $\tau_2 = 8.24$ (80.0%)	52.5%
c_1	0.33, air	$\tau_1 = 0.26$ (39.2%) $\tau_2 = 1.23$ (60.8%)	$\tau_1 = 0.77$ (42.5%) $\tau_2 = 4.96$ (57.5%)	71.5%

[a] All samples are C12A7:0.5%Eu^{3+} powders. Sample a is as-prepared, b, c and d are treated in 20% H_2/80% N_2 atmosphere at 1300 °C. c_1 represents the sample c with further treatment in air at 400 °C. [b] Emission decay of $^5D_0 \rightarrow {}^7F_2$ transition of Eu^{3+}. [c] Emission decay of 5d → 4f transition of Eu^{2+}. [d] The quantum yields of samples are obtained under excitation at 255 nm.

0.18 ms, respectively. This decrease can be ascribed to the production of more OH^-, accelerating the nonradiative transition process in all Eu^{3+} because the energy separation of $^5D_0 \rightarrow {}^7F_6$ is about 3 times the OH^- vibration frequency. For the annealed samples, the similar decay times of Eu^{3+} indicate that the environment around the unreduced Eu^{3+} remains unchanged. On the other hand, with increasing the annealing time, the quantum yields increase from 12.7% to 52.5% as listed in Table 1. This increase can be mainly attributed to the larger ratio of Eu^{2+} to Eu^{3+} after the annealing.

Fig. 7 illustrates the FTIR transmittance spectra of the as-prepared and annealed C12A7:Eu. The broad band peaked at 3426 cm^{-1} originates from the absorption of water adsorbed on KBr media and C12A7 powder surface. The stretching mode of encaged OH^- ions peaked at 3600 cm^{-1} is found to shift to 3520 cm^{-1} as the annealing time increases, suggesting the interaction among encaged OH^- ions is becoming non-negligible as a result of the increased production of OH^-, which is in agreement with the analysis of the emission decays of Eu^{3+}.

On the other hand, Fig. 8 shows the luminescence decays of the 5d–4f transition of Eu^{2+} monitored at 438 nm with excitation at 255 nm and the fitting results are also listed in Table 1, where the decay of Eu^{2+} demonstrates different behaviour in comparison with that of Eu^{3+}. Although the emission decay of Eu^{2+} can be divided into two time constants as well, the long and short components of Eu^{2+} can be ascribed respectively to the existence of two different local environments of H^- and O^{2-}, instead of O^{2-} and OH^- as in the case of Eu^{3+}. As the annealing time increases, the emission decays of Eu^{2+} increase from 5.45 to 8.24 μs for the long component and from 0.84 to 1.14 μs for the short component. This trend can be explained by the fact that formation of more encaged H^- leads to a higher local symmetry of Eu^{2+}. Thus it decreases the radiative transition rates and increases the lifetime due to the d-electron

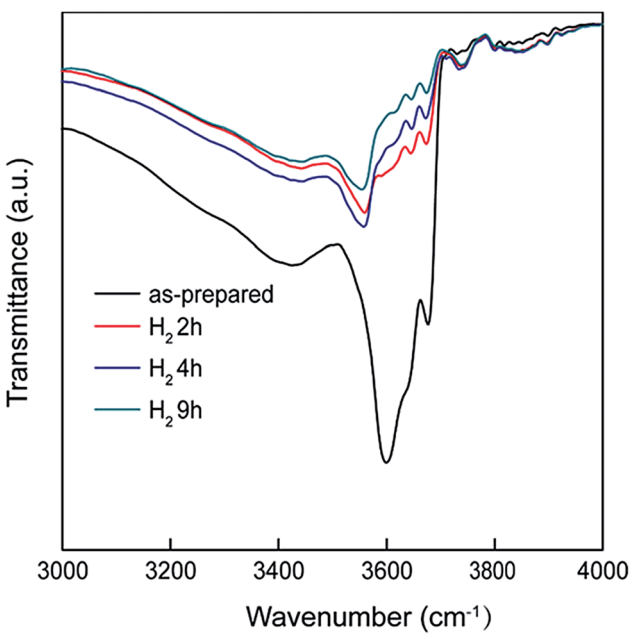

Fig. 7 FTIR transmittance spectra of C12A7:0.5%Eu^{3+} annealed in H_2/N_2 atmosphere for different times.

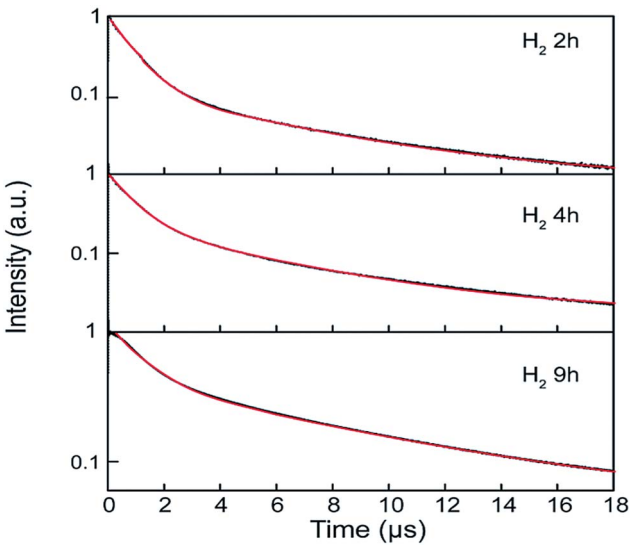

Fig. 8 Decay curves of Eu^{2+} monitoring at 438 nm and excited at 255 nm. The red line represents the best fit to data using a bi-exponential function.

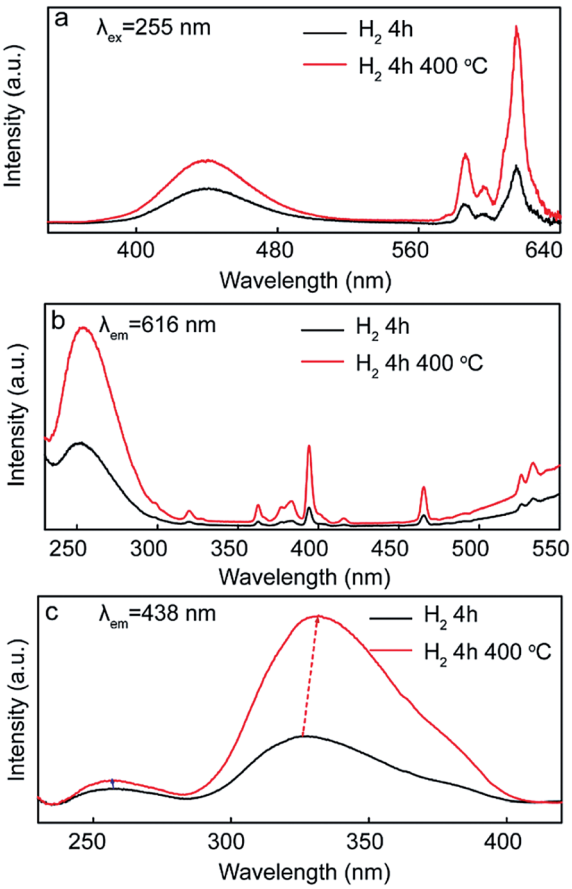

Fig. 9 Emission and excitation spectra of C12A7:Eu^{3+} annealed in H_2/N_2 atmosphere for 4 h (black) and the sample then treated in air at 400 °C for 0.33 h (red). (a) $\lambda_{ex} = 255$ nm, (b) $\lambda_{em} = 616$ nm and (c) $\lambda_{em} = 438$ nm.

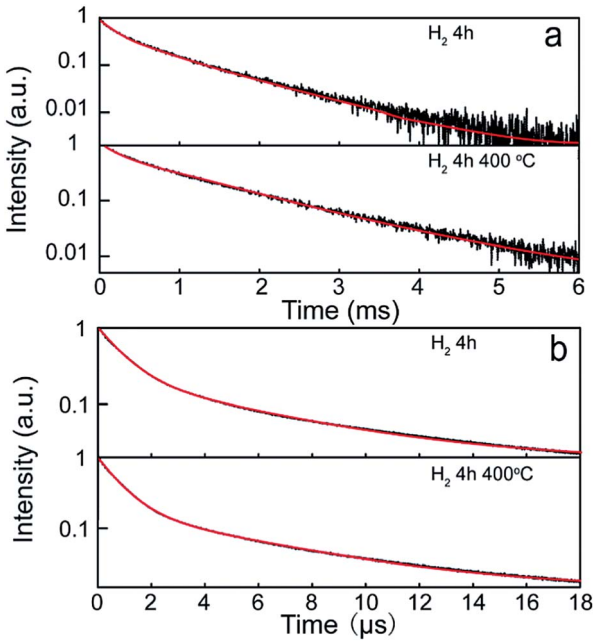

Fig. 10 (a) Decay curves of Eu^{3+} monitored at 616 nm and (b) Eu^{2+} monitored at 438 nm of C12A7:Eu^{3+} annealed in H_2/N_2 atmosphere for 4 h and the sample then treated in air at 400 °C for 0.33 h. Excitation is at 255 nm. The red line represents the best fit using a bi-exponential function.

characteristic in Eu^{2+}, which is sensitive to the local environments. The above results are in good agreement with that reported by Baran *et al.*, where Eu^{2+} and Eu^{3+} were codoped in tricalcium diyttrium trisilicon oxide, the symmetry and crystal field of active centres were modified at high pressure and the change of decay rates for both 5d–4f (Eu^{2+}) and $^5D_0$–^7F_J (Eu^{3+}) transitions observed.[29] Because it is easier for Eu^{3+} in the vicinity of O^{2-} to be converted into Eu^{2+} than that with OH^- in the locality, H^- will distribute around Eu^{2+} with more probability when H^- and OH^- are created equally after the annealing. The luminescence spectra have been modulated by changing the encaged anions through the annealing under H_2 atmosphere. The modulation can also be demonstrated by treating the annealed samples in air, where some encaged OH^- and H^- are expelled by O^{2-} through the reaction described by eqn (1) reversibly. Fig. 9a represents the emission spectra of the sample annealed for 4 h earlier then treated in air at 400 °C for 0.33 h under the excitation of 255 nm. Both the enhanced luminescence of Eu^{3+} and Eu^{2+} can be observed after treatment at 400 °C. Usually, the oxidization of Eu^{2+} in air will result in the decrease of the Eu^{2+} luminescence intensity. The abnormal increase of Eu^{2+} may be ascribed to the amount change of encaged anions which will be discussed in the following emission decays. Fig. 9b and c depict the corresponding excitation spectra. When monitoring 438 nm emission of Eu^{2+}, blue- and red-shifts of excitations at 255 and 326 nm, respectively, are observed after the treatment in air. It is in accordance with the observation in Fig. 5a, suggesting that the reaction described by eqn (1) occurs reversibly.

The corresponding luminescence decays of the $^5D_0 \rightarrow {}^7F_2$ transition of Eu^{3+} and that of the 4f → 5d transition of Eu^{2+} are given in Fig. 10a and b, and the fitting results are listed in Table 1 (last row). After treatment in air, the lifetimes of both the long and short components of Eu^{3+} increase, while those of Eu^{2+} nearly remain unchanged. Here, there are two factors to affect the lifetimes of Eu^{3+} and Eu^{2+}. They are the lower crystal field symmetry and the absence of encaged OH^-, respectively, caused by expelling encaged OH^- and H^- by encaged O^{2-}. The lower crystal field symmetry will increase the radiative transition rate or shorten the lifetime, as verified from the increase of the integrated intensity ratio of the $^5D_0$–$^7F_2$ to $^5D_0$–$^7F_1$ emissions from 2.7 (4 h H_2 annealed) to 2.9 (air treated). The absence of encaged OH^- will decrease the nonradiative transition rate and prolong the lifetime. For Eu^{3+}, because it is insensitive to the local environment, the absence of encaged OH^- plays a dominating role on its lifetime and prolongs the decay. For Eu^{2+}, it is sensitive to the local environment due to its d-electron characteristics, so the opposite variation tendency of the lifetimes caused by the two factors results in the nearly constant lifetimes of Eu^{2+}. The above results suggest that the luminescence of C12A7:Eu can be modulated by tuning the nonradiative and radiative transition rates, realized by controlling the sort and amount of the encaged anions. When the H_2 annealed sample was treated in air, the quantum yield increases from 29.4% to 71.5% (last column in Table 1) due to the decrease of

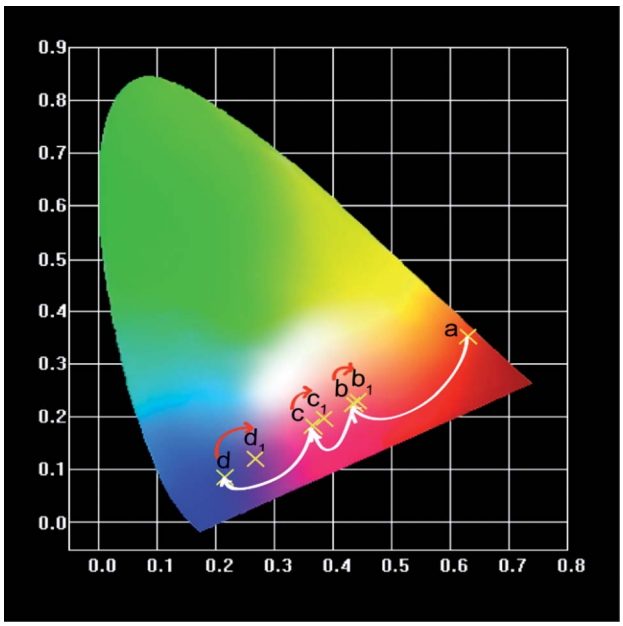

Fig. 11 Dependence of the CIE chromaticity coordinates on different heat treatment conditions, as listed in Table 1 and 2, for C12A7:Eu under 255 nm excitation.

Table 2 The CIE chromaticity coordinates of C12A7:Eu under different annealing conditions

Sample[a]	Heating (h) (H_2 or air)	CIE chromaticity
a	As-prepared	(0.630, 0.352)
b	2, H_2	(0.435, 0.225)
b_1	0.33, air	(0.443, 0.231)
c	4, H_2	(0.366, 0.183)
c_1	0.33, air	(0.386, 0.198)
d	9, H_2	(0.216, 0.086)
d_1	0.33, air	(0.267, 0.119)

[a] All samples are C12A7:0.5%Eu^{3+} powders. Sample a is as prepared, b, c, and d are treated in 20% H_2/80% N_2 atmosphere at 1300 °C. b_1, c_1, d_1 in air at 400 °C following the previous treatment for the corresponding samples.

nonradiative transition and the increase of radiative transition rate, as discussed above.

To demonstrate the power of this strategy, we have modulated the colour of CIE coordinates of C12A7:Eu upon a single wavelength excitation at 255 nm. The result is shown in Fig. 11 and summarized in Table 2. The fine colour tuning of C12A7:Eu phosphor from red (0.630, 0.352) to blue (0.216, 0.086) is successfully realized. This change is also reversible to some extent when treating the samples in air. The spectral modulation is then realized through changing the radiative (for Eu^{2+}) and nonradiative (for Eu^{3+}) channels of two emission centres in one system.

4. Conclusions

In conclusion, a fine colour tuning concept has been proposed and validated in C12A7:Eu phosphor through simultaneously modulating the radiative and nonradiative channels of Eu^{2+} and Eu^{3+} centres. It is based on the control of the encaged anions in C12A7 due to its unique nanocage structure. Both blue (Eu^{2+}) and red (Eu^{3+}) emissions are simultaneously generated upon a single wavelength excitation at 255 nm. Varying the annealing duration, the CIE chromaticity coordinates are tuned from (0.630, 0.352) to (0.201, 0.086). This concept can be readily extended to other rare earth or transition metal ions doped in C12A7 and be helpful for designing LEDs and novel optical materials.

Acknowledgements

This work was supported by the National Natural Science Foundation of China (no. 11374047, no.11074031, no. 11304036), the 111 Project (no. B13013), the Program for Century Excellent Talents in University (no. NCET-08-0757), the Fundamental Research Funds for the Central Universities (no. 12SSXM001, no. 10QNJJ008), the National Basic Research Program of China (973 Program) (no. 2012CB933703), the exchange program between CAS of China and KNAW of the Netherlands, and IOP program of the Netherlands and John van Geuns foundation. We gratefully thank Prof. Hongwei Song of Jilin University for the help in data collection of the emission decays and Prof. Jun Lin of Changchun Institute of Applied Chemistry for the assistance in quantum yield measurement.

Notes and references

1 K. Bando, K. Sakano, Y. Noguchi and Y. Shimizu, *J. Light Visual Environ.*, 1998, **22**, 2–5.
2 T. Taguchi, *IEEJ Trans. Electr. Electron. Eng.*, 2008, **3**, 21–26.
3 S. Pimputkar, J. S. Speck, S. P. DenBaars and S. Nakamura, *Nat. Photonics*, 2009, **3**, 180–182.
4 A. A. Setlur, W. J. Heward, Y. Gao, A. M. Srivastava, R. G. Chandran and M. V. Shankar, *Chem. Mater.*, 2006, **18**, 3314–3322.
5 X. F. Li, J. D. Budai, F. Liu, J. Y. Howe, J. H. Zhang, X. J. Wang, Z. J. Gu, C. J. Sun, R. S. Meltzer and Z. W. Pan, *Light: Sci. Appl.*, 2013, **2**, e50.
6 Z. Y. Mao, D. J. Wang, Q. F. Lu, W. H. Yu and Z. H. Yuan, *Chem. Commun.*, 2009, 346–348.
7 Z. Y. Mao and D. J. Wang, *Inorg. Chem.*, 2010, **49**, 4922–4927.
8 U. V. Varadaraju, K. A. Thomas, B. Sivasankar and G. V. S. Raoa, *J. Chem. Soc., Chem. Commun.*, 1987, **11**, 814–815.
9 J. Gopalakrishnan and K. K. Rangan, *Chem. Mater.*, 1992, **4**, 745–747.
10 M. A. Talbi, R. Brochu, C. Parent, L. Rabardel and G. L. Flem, *J. Solid State Chem.*, 1994, **110**, 350–355.
11 M. P. Saradhi, V. Pralong, U. V. Varadaraju and B. Raveau, *Chem. Mater.*, 2009, **21**, 1793–1795.
12 K. W. Huang, W. T. Chen, C. I. Chu, S. F. Hu, H. S. Sheu, B. M. Cheng, J. M. Chen and R. S. Liu, *Chem. Mater.*, 2012, **24**, 2220–2227.
13 K. Hayashi, S. Matauishi, T. Kamiya, M. Hirano and H. Hosono, *Nature*, 2002, **419**, 462–465.

14 K. Hayashi, P. V. Sushko, D. M. Ramo, A. L. Shluger, S. Watauchi, I. Tanaka, S. Matsuishi, M. Hirano and H. Hosono, *J. Phys. Chem. B*, 2007, **111**, 1946–1956.
15 X. L. Liu, Y. X. Liu, D. T. Yan, H. C. Zhu, C. G. Liu, C. S. Xu, Y. C. Liu and X. J. Wang, *J. Mater. Chem.*, 2012, **22**, 16839–16843.
16 G. J. Gao, S. Reibstein, M. Y. Peng and L. Wondraczek, *J. Mater. Chem.*, 2011, **21**, 3156–3161.
17 Y. G. Su, L. P. Li and G. S. Li, *Chem. Mater.*, 2008, **20**, 6060–6067.
18 H. W. Song, B. J. Chen, H. S. Peng and J. S. Zhang, *Appl. Phys. Lett.*, 2002, **81**, 1776–1778.
19 X. M. Liu, C. K. Lin and J. Lin, *Appl. Phys. Lett.*, 2007, **90**, 081904.
20 K. Hayashi, N. Ueda, M. Hirano and H. Hosono, *Solid State Ionics*, 2004, **173**, 89–94.
21 K. Hayashi, S. Matsuishi, M. Hirano and H. Hosono, *J. Phys. Chem. B*, 2004, **108**, 8920–8925.
22 M. Ruszak, S. Witkowski and Z. Sojka, *Res. Chem. Intermed.*, 2007, **33**, 689–703.
23 T. Iwata, M. Haniuda and K. Fukuda, *J. Solid State Chem.*, 2008, **181**, 51–55.
24 M. Zeuner, F. Hintze and W. Schnick, *Chem. Mater.*, 2009, **21**, 336–342.
25 M. Zeuner, P. J. Schmidt and W. Schnick, *Chem. Mater.*, 2009, **21**, 2467–2473.
26 N. Avci, K. Korthout, M. A. Newton, P. F. Smet and D. Poelman, *Opt. Mater. Express*, 2012, **2**, 321–330.
27 P. V. Sushko, A. L. Shluger, M. Hirano and H. Hosono, *J. Am. Chem. Soc.*, 2007, **129**, 942–951.
28 S. W. Kim, S. Matsuishi, T. Nomura, Y. Kubota, M. Takata, K. Hayashi, T. Kamiya, M. Hirano and H. Hosono, *Nano Lett.*, 2007, **7**, 1138–1143.
29 A. Baran, S. Mahlik, M. Grinberg and E. Zych, *J. Phys.: Condens. Matter*, 2013, **25**, 025603.